



Cite this: *Soft Matter*, 2023, 19, 7020

Received 2nd June 2023,  
Accepted 9th August 2023

DOI: 10.1039/d3sm00720k

[rsc.li/soft-matter-journal](http://rsc.li/soft-matter-journal)

## Plant-based, aqueous, water-repellent sprays for coating textiles†

Sara K. Fleetwood,<sup>id</sup><sup>a</sup> Sydney Bell,<sup>id</sup><sup>b</sup> Reinhard Jetter<sup>id</sup><sup>bc</sup> and E. Johan Foster<sup>id</sup><sup>\*a</sup>

Novel superhydrophobic coatings, that are both biodegradable and biosourced, have the potential to revolutionize the water-repellent coating industry. Here, water-repellent coatings were prepared from commercially unavailable plant waxes, isolated using solvent extraction and characterized using DSC, GC-MS and DLS. In the first stage, a plant survey was conducted to identify an ideal plant source for the final spray, in which Whatman filter paper was submerged in a wax-solvent solution with recrystallization occurring upon air-drying. In the second stage, aqueous, PFC-free wax dispersions were prepared, coated onto textiles (cotton and polyester), and heat-treated with a home drying machine to allow for the spreading and recrystallization of the waxes. In both stages, SEM visualization verified the coating's morphology, and contact angle measurements showed them to be superhydrophobic. It was concluded that, using less coating material than commercial coatings, high-performing petroleum-free coatings could be made and applied onto textiles of various polarities.

## 1 Introduction

Superhydrophobic coatings (contact angle  $>150^\circ$ ) have gained significant attention in recent years due to their ability to make a wide variety of materials self-cleaning, anti-fogging, and/or anti-biofouling. Therefore, superhydrophobic coatings are useful in a plethora of applications, including rainwear, solar panels, skis, produce, cars, *etc.* To stay dry and allow thermo-regulation of the body, outdoor users currently apply commercial water-repellent sprays, or durable water-repellent coatings (DWR), to their apparel and gear (ex. rainjacket, shirt, softshell, tent) at home by spraying and then heat treating in their drying machine. This prevents the fabric from becoming saturated with water, which prevents discomfort or hypothermia by reducing the heat transfer away from the body caused by evaporative cooling. However, to minimize environmental impact, these coatings need to also be durable, non-toxic, and biodegradable.

Water-repellent coatings typically contain perfluorinated compounds (PFCs), or more specifically perfluoroalkyl substances

(PFASs), due to their low surface energy. However, PFASs with long chain lengths of seven or more carbons accumulate within the body and do not break down in the environment.<sup>1</sup> Therefore, there has been a shift to using shorter perfluoroalkyls with C4 to C6 chains. While shorter fluorinated chains are not considered to bioaccumulate, they persist in the environment, their key performance characteristics are not as good, and there is a lack of long-term data on their impact on the environment and human health.<sup>2</sup> For these reasons, concerns of using long-chain PFASs began in the 1960s, and a growing number of restrictions have since been put on the use of these chemicals, with the outdoor apparel industry receiving some of the most scrutiny as a route of exposure to PFASs.<sup>3</sup> This has led to large companies such as Arc'teryx and Patagonia posting PFC-free and PFAS-free statements on their websites<sup>4,5</sup>:

“PFC-free DWR is a serious focus for our R&D efforts . . . To date, all of the non-PFC DWR treatments we have tested have fallen short.”<sup>4</sup>

Environmental and human health concerns for water-repellent coatings using PFAS chemistry have led to the exploration of PFC-free chemistries,<sup>3</sup> one solution being waxes. However, the processes used are often not industrially scalable, use complex chemical compositions (negating the benefits of being plant-based), and/or cannot be applied by users at home. Common techniques for dispersing waxes in surfactants include homogenization, either by rotor-stator or high-pressure and ultrasonication, or dispersing in organic alcohols through self-emulsification.<sup>6</sup> A more environmentally friendly alternative would be to use an aqueous wax suspension.

<sup>a</sup> Department of Chemical and Biological Engineering 421, University of British Columbia, 2360 East Mall, Vancouver, BC V6T 1Z3, Canada.

E-mail: [johan.foster@ubc.ca](mailto:johan.foster@ubc.ca)

<sup>b</sup> Department of Chemistry, University of British Columbia, 2036 Main Mall, Vancouver, BC V6T 1Z1, Canada

<sup>c</sup> Department of Botany, University of British Columbia, 6270 University Boulevard, Vancouver, BC V6T 1Z4, Canada

† Electronic supplementary information (ESI) available. See DOI: <https://doi.org/10.1039/d3sm00720k>



However, past literature has stated that to stabilize this would require 10% or more emulsifier.<sup>7</sup> However, adding more emulsifier can increase the surface energy of the particles, thus reducing waterproof properties.<sup>6,8</sup>

A few papers have reported aqueous wax dispersions without emulsifiers, all using non-scalable techniques to create the suspension or apply it to the surface. These waxes were either petroleum based, made of a combination of beeswax and carnauba wax, or incorporated nanoparticles into their coating. For example, Bayer *et al.* spray casted surfactant-free wax-in-alcohol (carnauba wax in isopropyl alcohol or ethanol) emulsions containing suspended ~150 nm PTFE nanoparticles (prepared using sonication) onto glass slides, followed by thermal annealing on a hot plate at 110 °C for 15 min to achieve superhydrophobic surfaces with 150 µm film thicknesses and PTFE/wax mass fractions >0.6.<sup>7</sup> Lozhechnikova *et al.* took this a step further and prepared an aqueous self-emulsifying carnauba wax layer-by-layer (LBL) coating using probe sonication.<sup>6</sup> Forsman *et al.* used LBL deposition of cationic poly-L-lysine and anionic carnauba wax particles (wax dispersion prepared *via* probe sonication) to coat linen and cotton, followed by thermal annealing in an oven at 103 °C for 1 h to achieve superhydrophobicity for the two bilayers (2BL) sample on light cotton.<sup>9</sup> Wang *et al.* spray coated wax-in-acetone emulsions of carnauba wax and beeswax (prepared using ultrasonication) onto glass slides and polystyrene cups for easy removal of food container residues to reduce food waste, achieving superhydrophobicity with surface densities of carnauba wax  $\geq 0.55 \text{ mg cm}^{-2}$ .<sup>10</sup>

Within industry, mountainFLOW Eco Wax LLC has developed plant-based waxes for applying to skis and bikes, including an aqueous dispersion that can be sprayed onto ski skins. However, all of their patents pertain to melting solid blocks of plant wax onto skis as the intended use, rather than applying to outdoor apparel and gear that is intended to keep the user dry. Additionally, their chemical composition uses commercially available plant waxes, with the primary contents being either candelilla, carnauba, rice bran, or castor wax.<sup>11,12</sup>

In all scientifically reported and industrially used systems, the waxes were petroleum-based (ex. paraffin wax) or obtained from commercially available biological sources. Among the biologically sourced waxes, beeswax, carnauba, candelilla, and sugarcane are economically the most important, while ouricury, esparto, bamboo, rice bran, and Japan wax are of local importance.<sup>13</sup> Carnauba wax is a natural ester wax found on the leaves of the carnauba palm, *Copernicia prunifera*, which is only grown in northeastern Brazil. It is a common leaf wax used in commercial applications, as it is one of the hardest natural waxes and has a high melting point of 82.0–85.5 °C. Carnauba wax consists primarily of wax alkyl esters (40%) of acids with average chain length C<sub>26</sub> and alcohols with average chain length C<sub>32</sub>.<sup>13</sup> Often, carnauba wax is mixed with beeswax, which has a lower melting point of 62–65 °C,<sup>13</sup> to reduce brittleness.

Carnauba palms are evergreens, meaning their leaves must be harvested for wax extraction. To keep the tree healthy, only 20–30 leaves can be harvested per tree each year.<sup>14</sup> Instead, it

would be better to use waxes from plant waste streams, such as leaf-litter from deciduous plants or conifer needles from slash piles that remain in the forest after logging. Many plants coat their leaves or needles with waxes composed of large amounts of nonacosan-10-ol and nonacosanediols.<sup>15</sup> These two compound types are known to spontaneously co-crystallize into nanotubules, a structure that allows the hydrophilic hydroxyl groups to be buried between layers and the hydrophobic methyl groups to form the external surface of the tubules.<sup>16</sup> Because of the nano-roughness they add to the surface of the plant, nanotubules can achieve much higher contact angles than smooth wax films (*e.g.*, in the Lotus effect). Moreover, nanotubules give similar contact angles to wax platelets but do so more efficiently, due to higher surface-to-volume ratios and require fewer co-crystallizing compounds for crystal formation to occur. Currently, tubular waxes are not commercially available, as their plant sources have in the past been considered to produce minute quantities of wax in comparison to other sources.<sup>14</sup>

Herein, we explored using commercially unavailable, tubule-forming plant waxes to produce novel water-repellent coatings for applying to textiles. Through the preparation of these aqueous wax suspensions, we aimed to improve the scalability of the process by using a homogenizer in place of probe sonication. Additionally, we aimed to produce a stable coating using no emulsifiers that could be applied as a single-layer spray-on coating and, with the addition of heat from a home drying machine, would recrystallize into tubules. In doing so, a simpler, two-step coating process would be developed, allowing for coatings to be applied at home. It was anticipated that, by using wax sources containing the secondary alcohol nonacosan-10-ol, the hydrophobicity of this coating would be comparable or greater than that of commercial products, thus producing a petroleum- and PFC-free alternative.

## 2 Experimental methods

### 2.1 Materials

Leaves were collected from maple (*Acer rubrum*), horsetail (*Equisetum arvense*, sterile shoots), ginkgo (*Ginkgo biloba*), katsura (*Cercidiphyllum japonicum*), cedar (*Cedrus atlantica*), and smoketree (*Cotinus coggygria*) plants growing on the University of British Columbia campus (Vancouver, Canada) (Fig. 6). 100% pure carnauba wax of T1 Grade was purchased from H&B Oils Center Co. Chloroform (ACS reagent), *N,O*-bis(trimethylsilyl)trifluoroacetamide (BSTFA) (GC derivatization, LiChropur™,  $\geq 99.0\%$ ), and hexanes (ACS Reagent) were purchased from Sigma-Aldrich (St. Louis, United States of America). *n*-Tetracosane ( $\geq 99\%$ ) was purchased from Alfa Aesar (Ward Hill, United States of America). Pyridine (ACS Reagent) was purchased from Caledon (Georgetown, Canada). Helium ( $\geq 99\%$ ), hydrogen ( $\geq 99.95\%$ ) and nitrogen ( $\geq 99.998\%$ ) were purchased from Linde (Mississauga, Canada).

Commercial spray-on coatings were purchased directly from the manufacturer's website or through online retailers. Grangers Performance Repel Plus (OWP) is produced in the UK,



marketed for use on waterproof clothing, and is PFC-free. Nikwax SoftShell Proof™ Spray-On is also produced in the UK, marketed for use on softshells, and is water-based, PFC-free, and non-petroleum based. Arc'teryx N $\mu$  is a re-branded product of Gear Aid (Bellingham, United States of America), marketed for use on technical outerwear fabrics (including GORE-TEX, softshells and windshells), and contains PFCs, and is petroleum-based. Fjäll Räven Waterproofing Impregnation is produced in Sweden, marketed for use on waterproof/breathable apparel, PFC-free, and contains petroleum based products such as polyurethane. Throughout the remainder of the paper these will be randomly assigned and referred to by the names “Coating 1–4”, respectively.

Hydrophilic and hydrophobic material substrates were used for applying the coatings. Grade 40 Whatman filter paper (100% cotton, nominal pore size 8  $\mu$ m) was purchased from Fisher Scientific (Waltham, United States of America) and will be referred to as “filter paper” throughout the remainder of the paper. 100% cotton twill (0900801 Cotton Twill, 006 greige) and 100% polyester knit (039400 Scuba, 008 off white) were purchased from Fabricland Online (Toronto, Canada). A t-shirt made of 100% organic cotton jersey (birch white) was purchased from Patagonia, Inc. (Ventura, United States of America). A t-shirt made of 100% recycled polyester spun jersey (classic navy) was purchased from Patagonia, Inc. (Ventura, United States of America). All fabric was first washed with Seventh Generation Laundry Detergent (Fresh Lavender Scent) and then dried.

## 2.2. Overview of plant wax extraction methods

Plant waxes were extracted using three different methods: (1) small lab-scale (Section 2.3.1), (2) large-scale (Section 2.4.1), and (3) analytical-scale (Section 2.5.6), which are described in further detail in their corresponding sections. A detailed graphic of process steps for the plant survey (Section 2.3) and the scale-up experiments (Section 2.4 and 2.5) are shown in Fig. 1.

## 2.3 Plant wax survey

**2.3.1 Laboratory-scale wax isolation.** Leaves and needles were cut from plants and immediately rinsed in reverse osmosis (RO)-purified water three times, using a fresh batch of water each time, to remove any particulate. Wax was extracted from

leaves and needles by immersing individual leaves or 5 g of needles in 100  $\times$  15 mm glass pyrex dishes containing chloroform for 5 min. Chloroform was removed by evaporating in the fume hood for approximately 24 hours, leaving solid wax in the pyrex dish.

**2.3.2 Coating Whatman filter paper (i.e. cotton) by soaking.** Chloroform was added to the pyrex Petri dish containing plant wax (all, except carnauba wax) to create a concentration of a 5 mg mL<sup>-1</sup> wax solution. Carnauba wax was difficult to dissolve in chloroform, so the pyrex dish was covered and placed on a hot plate, externally set at 90  $^{\circ}$ C, for 10 min in order to dissolve the wax faster. 2  $\times$  2 cm<sup>2</sup> squares of filter paper were placed in the dish and soaked for 5 min. Upon removal, the filter paper was held horizontally in the air for 1 min to allow the chloroform to evaporate from the filter paper.

## 2.4 Scaling-up isolation and coating processes

**2.4.1 Large-scale wax isolation.** For large-scale experiments, leaf litter was collected from the ground in fall and rinsed in RO-purified water three times, using clean water each time, to remove any particulate. Wax was extracted from batches of 50 and 100 leaves, respectively, in 170  $\times$  90 mm and 254  $\times$  381 mm pyrex glass dishes filled with chloroform and mixed for 5 min with a magnetic stir bar. Chloroform was recycled under reduced pressure using a roto-vap and reused on the same plant species. Residual chloroform was evaporated at room temperature for 24 hours, leaving solid wax in the pyrex dish. Wax was then redissolved in a small amount of chloroform and transferred into a smaller pyrex dish.

**2.4.2 Suspension for hydrophobic spray.** The coating material was prepared with 0.01 g mL<sup>-1</sup> wax-RO water (containing no emulsifiers) in a 250 mL flask, which was heated in boiling water until the wax fully melted. The mixture was then homogenized for 30 min at 15 000 rpm, using an IKA (Staufen, Germany) T25 Ultra-Turrax Homogenizer, mounted with a S25 N-18G Dispersing Tool. Subsequently, the emulsion was quenched in an ice bath and filtered through a filter funnel, containing a 40–90  $\mu$ m nominal maximal pore size fritted disc. The wax particles then solidified and the emulsion became a suspension.

**2.4.3 Coating textiles by spraying.** 0.01 g mL<sup>-1</sup> suspensions were poured into Dynalon Flip & Spray Bottles. 4  $\times$  4 cm<sup>2</sup>

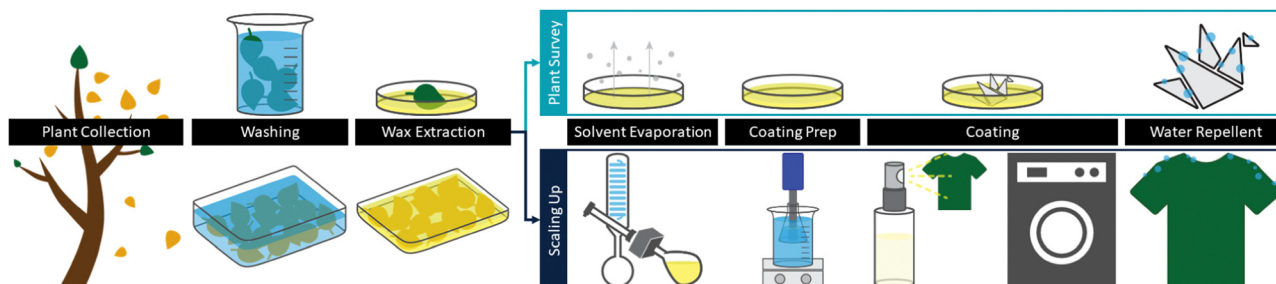


**Fig. 1** Wax isolation process and coating preparation for the plant survey (Section 2.3) and scale up (Section 2.4). The process began by collecting leaves or needles, washing in water, and then extracting wax using chloroform. During the plant survey, coating was done by submerging Whatman filter paper in a pyrex dish containing 0.005 g mL<sup>-1</sup> wax solution for 5 min and then air drying. During scale up, a 0.01 g mL<sup>-1</sup> aqueous suspension of wax was created, sprayed onto textiles, and then dried using air or heat (temperature-humidity chamber (“Tenney”) or home drying machine (“GE”).



squares of cotton and polyester fabric were then sprayed 10x each with the carnauba, or 5x each with the ginkgo wax suspensions, from a distance of 15 cm away. Samples were then dried using three different methods: (1) a Tenney T2RC Temperature/Humidity Cycling Chamber at 60 °C and 0% RH for 30 min, (2) GE 4 cu. ft. Electric Compact Dryer (model PCVH480EK0WW) on medium heat (~57.2 °C, timed dry) for 30 min, and (3) air drying overnight. Throughout the remainder of the paper, each drying method will be referred to as Tenney, GE dryer, and air dry.

For comparison, commercial coatings were also used to coat the substrates, following the instructions on their bottles. 4 × 4 cm<sup>2</sup> squares of cotton and polyester fabric were dipped in RO water to dampen, sprayed 20x from 15 cm away, and cleaned of excess coating by wiping after 2 min. Coating 2 and Coating 4 were dried with a GE 4 cu. ft. Electric Compact Dryer (model PCVH480EK0WW) on medium heat (~57.2 °C, timed dry) for 30 min, Coating 1 was dried on medium heat for 60 min, and Coating 3 was dried on low heat for 30 min.

Similar to the fabric squares, the suspension was poured into a Dynalon Flip & Spray Bottle, but was instead sprayed onto cotton and polyester t-shirts from a distance of 6 cm away. Samples were initially dried in the drying machine on medium heat for 30 min. However, this was not enough time for the t-shirts to completely dry, so t-shirts were dried for an additional 30 min on medium heat.

## 2.5 Characterization techniques

### 2.5.1 Wax extraction yield and coating weight percent.

Extracted wax yields were determined by weighing the pyrex dishes using a SECURA324-1S analytical balance when empty and then again after having added the wax-solvent solution, with the solvent fully evaporated. To calculate the wax extracted per leaf, the number of leaves to be used during wax extraction were counted. From this, the mg of wax/leaf could be calculated for each plant source.

The amount of coating applied to each substrate was determined by weighing the substrate before and after coating, allowing the coating to fully dry, and calculating the mass of wax per mass of substrate (wt%).

**2.5.2 Differential scanning calorimetry (DSC).** The thermal properties of waxes were measured using a TA Q1000 differential scanning calorimeter (DSC) with a nitrogen flow of 50 mL min<sup>-1</sup>. Sample masses of 6.0 mg were weighed<sup>17</sup> and loaded into 40 μL aluminum pans. Experiments began by equilibrating at 0 °C and holding this temperature for 5 min, followed by heating to 100 °C at a rate of 5 °C min<sup>-1</sup>, cooling to -20 °C, and then re-heating to 100 °C.<sup>18</sup> Thermograms of the first cooling and second heating were recorded.

### 2.5.3 Dynamic light scattering (DLS): dispersion stability.

All commercial samples and plant wax dispersions were first shaken rapidly for approximately 30 s. Commercial samples were diluted, but not filtered, for analysis using dynamic light scattering (DLS). Plant wax suspensions were prepared for DLS by filtering through a 0.45 μm Whatman GD/X syringe filter. Absorption values of plant waxes were acquired using a

Shimadzu UV-2600i UV-Vis Spectrophotometer. A Zetasizer Nano-ZS DLS was used to measure particle size distribution, polydispersity index (PDI), and Z-average, taking three measurements per sample, within one day and one month of sample preparation. The ζ-potential was calculated using the Smoluchowski model in the instrument software.

**2.5.4 Water contact angle (WCA).** Static water contact angle (WCA) measurements were performed using a Theta Flex 300-Pulsating Drop 200 Attension Tensiometer at room temperature. Approximately 10 μL MilliQ-purified water droplets were dispensed onto the coating substrate. A larger droplet volume (10 μL vs. 5 μL) was used to increase the droplet's weight, allowing the droplet to leave the pipette tip and be dispensed onto superhydrophobic sample surfaces.<sup>18</sup> Images of the droplet were taken at a frequency of 1.4 frames per second over 5 min, and analyzed using the Laplace-Young fitting mode in the Attension software to obtain WCAs. An increased contact time was used in order to better understand the performance of the coating with time.<sup>6</sup> For each coating, WCAs were measured on three or more locations of each sample.

**2.5.5 Scanning electron microscopy (SEM).** In preparation for imaging, samples were mounted on aluminum SEM stubs using non-conductive double-sided adhesive tape and sputter coated with ~10 nm of gold using a Cressington 208HR High Resolution Sputter Coater. SEM was carried out using a Hitachi S-2600 Variable Pressure SEM at an accelerating voltage of 5–6 kV, beam spot size of 10, working distance of 12 mm, and high vacuum.

### 2.5.6 Qualitative and quantitative analyses of wax extracts.

The total wax loads and relative abundances of compound classes were determined using GC-MS and gas chromatography-flame ionization detector (GC-FID). First, wax was extracted using a method suitable for analytical analysis. Extracted surface areas of needles were determined as described by Wen *et al.*,<sup>19</sup> using pixel counts of lengths and widths in ImageJ<sup>20</sup> and approximating needles as flat rectangles. The surface areas of the leaves were measured directly in ImageJ. Added to the leaves and needles was a defined quantity of *n*-tetracosane as an internal standard. The leaves and needles were then extracted with chloroform (3 × 20 mL), and the three solutions were combined.

Gas chromatography-mass spectrometry (GC-MS) was carried out following a procedure similar to Buschhaus and Jetter.<sup>21</sup> The wax was dissolved in 20 μL of pyridine, and then 20 μL of BSTFA was added. The solution was reacted at 70 °C for 45 min. Then, a stream of nitrogen gas at 60 °C was used to evaporate any excess derivatization reagent, and the residue was dissolved in 20 μL of chloroform. The derivatized wax samples were separated using GC (6890N, Agilent), equipped with an on-column injector and a HP-1 capillary column (Agilent; 30 m length, 320 μm i.d., 1 μm film thickness). An aliquot of the sample was injected on-column into a 2 mL min<sup>-1</sup> constant flow of hydrogen. The oven was held for 2 min at 50 °C, ramped to 200 °C at 40 °C min<sup>-1</sup>, held at 200 °C for 2 min, ramped to 320 °C at 3 °C min<sup>-1</sup>, and held at 320 °C for 30 min. A flame ionization detector (FID, Agilent) was used to quantitatively detect analytes, with flame settings of



20 mL per min nitrogen, 30 mL per min hydrogen and 200 mL per min air at 250 °C. The samples were analyzed qualitatively with the same GC and column setup, but a 1.4 mL min<sup>-1</sup> column flow of helium and a MS (5793N, Agilent, EI 70 eV, *m/z* 50–800, 1 scan s<sup>-1</sup>) were used instead.

To perform a GC-MS analysis of the commercial waterproofing sprays, a liquid–liquid extraction was performed for each spray by combining an aliquot of the spray (1 mL) with deionized water (3 mL) and hexanes (3 × 4 mL). The organic layers were combined and dried under a stream of nitrogen gas to yield the isolated waxy components. The isolated waxy components were derivatized and analyzed following the same procedure as the plant waxes.

## 3 Results and discussion

### 3.1 Plant wax survey: source wax properties

Initially, plant species were screened by visual inspection of water repelling properties, and trees with leaves appearing superhydrophobic were selected. This included leaves that were dry during rainstorms, appeared glaucous, caused water to bead on their surfaces, or appeared metallic when submerged in water (Fig. 2). The glaucous appearance is particularly of note, as this has been correlated to surface morphologies of high surface-to-volume ratios and high surface energies.<sup>22</sup>

To understand the impact of cuticular wax composition on contact angle and, thus, coating performance, waxes were extracted with chloroform from fresh leaves (maple, ginkgo, katsura, and smoketree), needles (cedar), or branches (horsetail) of the plant species with chloroform. The extracts were spiked with an internal standard (tetracosane), TMS-derivatized, and analyzed with GC-MS to identify individual wax components (Fig. S1–S6, ESI<sup>†</sup>). Common contaminants, such as GC column degradation products or environmental pollutants, were not included in the compound class analyses and wax quantifications.

The total wax coverages ranged from 2.6 μg cm<sup>-2</sup> in horsetail to 8.9 μg cm<sup>-2</sup> in smoketree, 15.7 μg cm<sup>-2</sup> in katsura, 19.1 μg cm<sup>-2</sup> in maple, 35.2 μg cm<sup>-2</sup> in ginkgo, and 76.8 μg cm<sup>-2</sup> in cedar (Fig. 3). Because surface areas were calculated using top-down projections assuming flat surfaces, wax coverages must be considered as approximations. In particular, cedar needles are fairly thick and may therefore have slightly larger surface areas and lower wax loads than estimated here.<sup>23</sup>

While the analytical extraction method used three washes, each with a duration of thirty seconds, the bulk extraction method used one wash with a duration of five minutes to



Fig. 2 Ginkgo leaves picked off the tree/fresh (green) and fallen/old (yellow). The left image shows the leaf dipped in water with a metallic sheen caused by the light reflecting off the air pockets formed between the water and waxy surface.

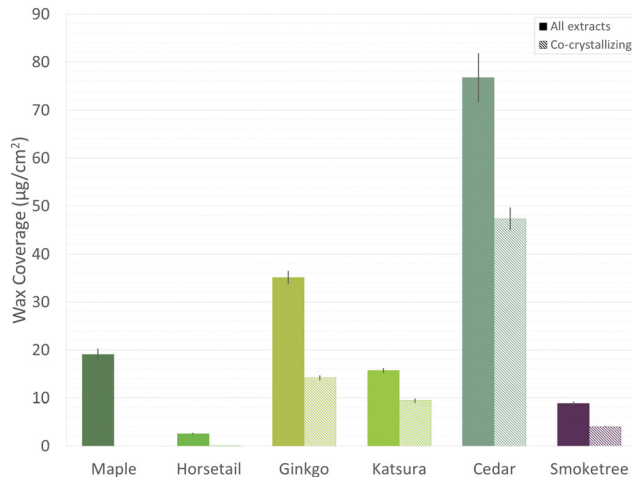


Fig. 3 Gas chromatography-mass spectrometry (GC-MS) survey of isolated plant waxes. The left column for each plant source (solid) shows the total wax coverage of the leaf/needle, the right column (hashed) shows the amount of nonacosan-10-ol and nonacosanediols thought to co-crystallize in nanotubules (averages ± s.e., *n* = 5). Common contaminants, such as column degradation byproducts or environmental pollutants, are excluded. Plant species: maple (*Acer rubrum*), horsetail (*Equisetum arvense*, sterile shoots), ginkgo (*Ginkgo biloba*), katsura (*Cercidiphyllum japonicum*), cedar (*Cedrus atlantica*), and smoketree (*Cotinus coggygria*).

reduce the relative amount of chloroform needed. It has been shown that, when submerged in chloroform, the majority of cuticular waxes are removed within ten seconds.<sup>24</sup> Using ginkgo as an example, it was determined that the bulk extraction method was able to achieve an extraction yield of about 43 μg cm<sup>-2</sup>. When adjusted for the difference in average leaf surface area between fresh leaves (66 cm<sup>2</sup>) as used in the analytical method and litter leaves as used in the bulk method (45 cm<sup>2</sup>), it was determined that the bulk method extracted about 80% of the wax that the analytical method achieved.

The wax analysis revealed a diversity of compound classes across the species. The most ubiquitous compound classes were the primary alcohols, secondary alcohols, and diols (Fig. 4). Only cedar wax had no detectable primary alcohols, and only maple wax had no detectable secondary alcohols or diols. Also frequently present were alkyl esters (found in cedar, smoketree, maple and horsetail waxes), aldehydes (maple, horsetail, and ginkgo), alkanes (smoketree, maple, and horsetail), and fatty acids (maple and horsetail). The more specialized compounds, alkyl acetates and hydroxyaldehydes, were only found in ginkgo wax. For brevity, the diverse cyclic compounds found in these species have been combined into one class (Table S1, ESI<sup>†</sup>).

The horsetail wax composition was dominated by primary alcohols (28%), and the maple wax was composed largely of alkanes (25%) and triterpenoids (24%). Secondary alcohols were the major component in cedar (54%), smoketree (42%), ginkgo (33%), and katsura (53%) waxes. In each of these four species, the most abundant compound was nonacosan-10-ol. These four species also all had diols present in their wax mixtures. In cedar, smoketree, and katsura, all the detected



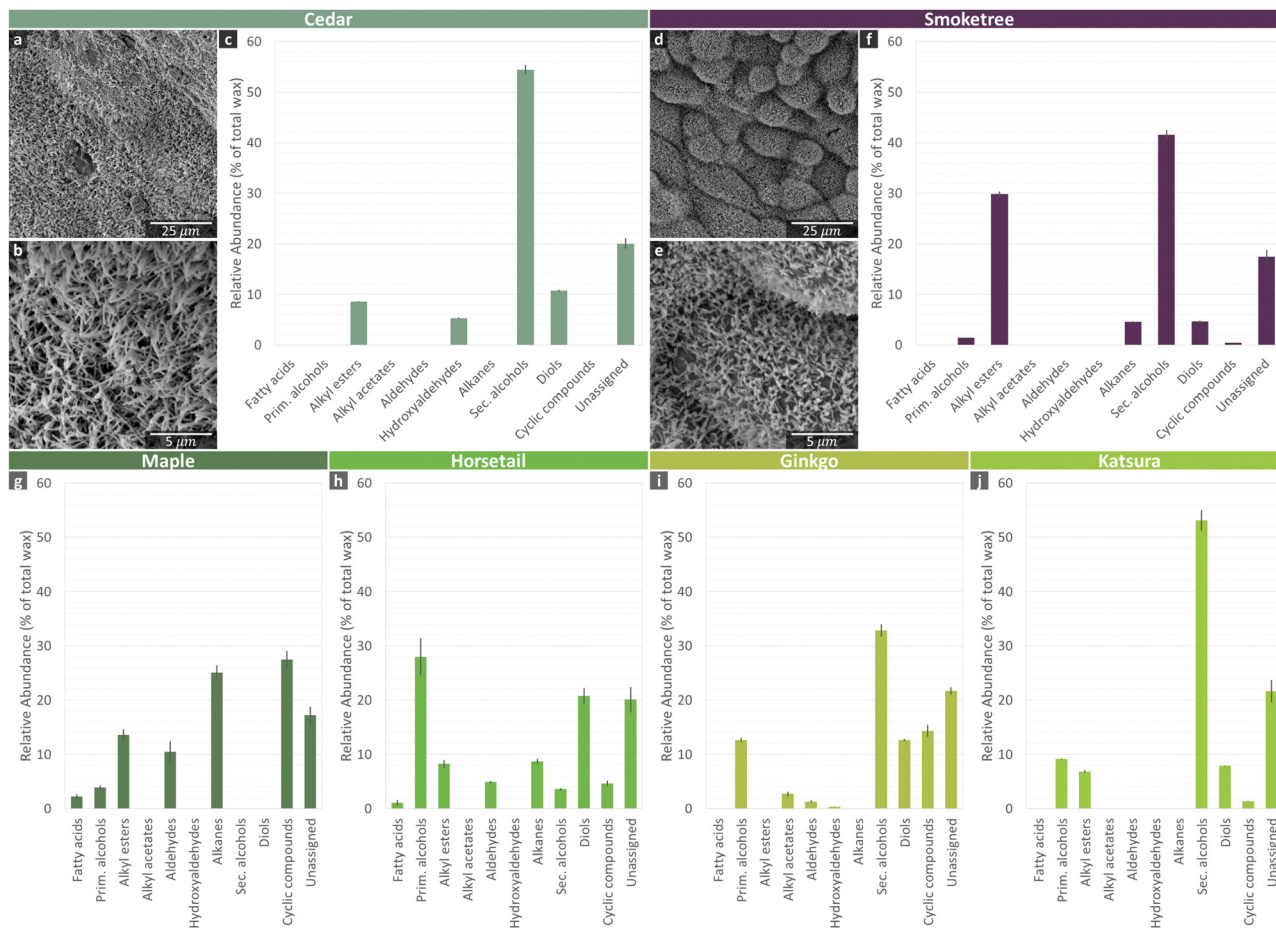


**Fig. 4** Chemical and micromorphological characterization of plant surface waxes. Gas chromatography-mass spectrometry (GC-MS) analysis of (c), (f), (g)–(j) isolated plant waxes showing the chemical composition of each wax as the relative abundance of compound classes. Also shown are scanning electron microscopy (SEM) images of the wax tubule surfaces of (a)–(b) conifer and (d) and (e) deciduous plant sources from the most hydrophobic samples, which also contained the largest abundance of secondary alcohols. Common contaminants, such as column degradation byproducts or environmental pollutants, are excluded. Plant species: cedar (*Cedrus atlantica*), smoketree (*Cotinus coggygria*), maple (*Acer rubrum*), horsetail (*Equisetum arvense*, sterile shoots), ginkgo (*Ginkgo biloba*), and katsura (*Cercidiphyllum japonicum*).

diols were 29 carbons long, but the most dominant hydroxyl group position varied from C-10/C-13 in cedar, to C-5/C-10 in smoketree, and C-4/C-10 in katsura. Interestingly, both a mid-chain-functionalized nonacosane-5,10-diol and terminally functionalized 1,3-diols (largely octacosane-1,3-diol) were found in ginkgo wax.

Maple, horsetail, smoketree, and ginkgo waxes have been described previously, and the findings of the present study generally agree with the literature. Further discussion on compounds found in comparison to prior literature can be found in the ESI.†

Nonacosan-10-ol and its diol derivatives are known to co-crystallize into wax tubules.<sup>15</sup> Thus, the combined total coverage of these compounds was also determined (Fig. 3). None of the co-crystallizing compounds were detected in maple and horsetail wax, while smoketree wax had  $4.05 \mu\text{g cm}^{-2}$  (45% of total wax), katsura wax had  $9.43 \mu\text{g cm}^{-2}$  (60% of total wax), ginkgo wax had  $14.16 \mu\text{g cm}^{-2}$  (40% of total wax), and cedar wax had  $47.30 \mu\text{g cm}^{-2}$  (62% of total wax).

The commercial waterproofing sprays were also screened with GC-MS to determine if any were made of common plant leaf waxes. Coating 2 consisted primarily of glyceryl palmitate, while the compositions of Coatings 1 and 4 were primarily erucamide. Glyceryl palmitate and erucamide can be found as natural products in plants, but neither are common leaf wax components. Coating 3 did not contain any compounds that are known to be plant leaf waxes.

The micro-morphologies of two of the more hydrophobic plant surfaces, cedar needles and smoketree leaves, were also investigated with SEM (Fig. 4), which showed tubular structures. These results match with previous reports on a closely related cedar species as well as smoketree.<sup>23,25</sup> Other plant waxes documented within the literature to have a tubular structure include ginkgo<sup>26</sup> and katsura.<sup>27</sup> Horsetail also has nano-scale surface roughness, but from silicon dioxide crystals.<sup>28</sup> In contrast, maple contains wax platelets<sup>29</sup> and the morphology of carnauba is not documented within the literature.



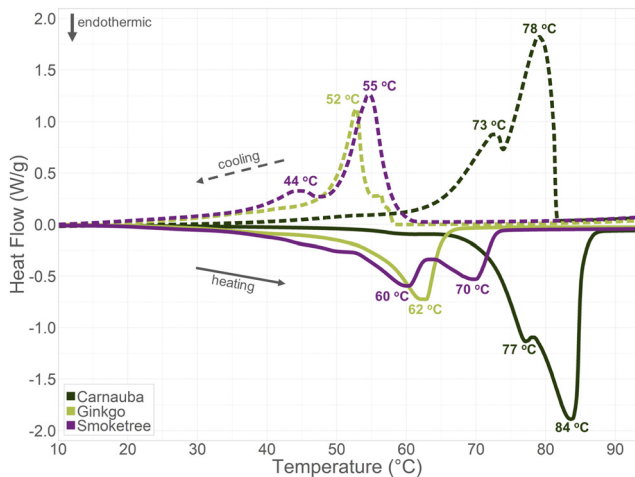


Fig. 5 Differential scanning calorimetry (DSC) heating and cooling thermograms of carnauba (*Copernicia prunifera*), smoketree (*Cotinus coggygria*), and ginkgo (*Ginkgo biloba*). A negative heat flow indicates an endothermic thermogram.

To determine the optimal temperature for melting of plant waxes and subsequently recrystallization, DSC measurements were taken (Fig. 5). Complete melting of carnauba, smoketree, and ginkgo waxes occurred at approximately 84, 70, and 62 °C respectively. Carnauba and smoketree waxes showed additional heat absorption peaks at roughly 77 and 60 °C, respectively. The additional heat absorption peaks of both waxes were likely due to polymorphic phase transitions, by which the wax mixtures existed in a semi solid–liquid form.<sup>10,18</sup> For the smoketree wax, considered to be non-pure, this is due to the melting of different components at different temperatures. Based on these DSC measurements, 60 °C was concluded to be a suitable temperature at which to anneal the fabric samples.

### 3.2 Plant wax survey: solvent-based wax coating performance

WCAs were measured to observe changes in hydrophobicity of the filter paper before and after coating. Control experiments showed that untreated filter paper immediately absorbed water, confirming its hydrophilic character. In contrast, all plant wax coated filter paper had WCAs greater than 120° (Fig. 6q), which is consistent with previous reports on wax-covered plant surfaces, where smooth wax layers had WCAs close to 90° and micro-structured waxes had WCAs in the range of 120–160°. <sup>30</sup> All plant waxes, except carnauba, held these WCAs for the full 5 min of testing, demonstrating their stability as hydrophobic coatings.

However, carnauba and maple waxes had considerably lower WCAs than the remainder of the plant waxes. Neither species waxes are known to contain secondary alcohols—carnauba waxes are reported to be mainly composed of alkyl esters,<sup>13</sup> and the present study found maple wax to be primarily alkanes and triterpenoids. Moreover, in reports on other species of maple, WCAs on the leaf fall significantly short of superhydrophobic. A tubule structure has not been reported for either wax, and red maple waxes are known to instead crystallize into platelets.<sup>13</sup>

The results for carnauba wax, exhibiting the lowest WCA and no surface nano-roughness, were particularly of interest, given that carnauba wax has been the focus of prior research on a plant-based alternative to PFC coatings due to its commercial availability and having a high melting point among plant waxes. Within 5 min, carnauba exhibited time-dependent wetting under the Cassie impregnating wetting regime.<sup>31</sup> Wetting may have been partially related to the relatively low solubility of carnauba wax, in comparison to other waxes, requiring the addition of heat during the coating procedure and possibly resulting in less uniform wax coverage.

The horsetail wax, which contained only traces of nonacosan-10-ol, but a significant amount of hentriacontane-6,8-diol, was capable of achieving near-superhydrophobicity on the filter paper. However, no wax crystals were visible using SEM.

The remaining waxes, ginkgo, katsura, cedar, and smoke-tree, all contained significant amounts of the co-crystallizing nonacosan-10-ol and nonacosanediols. Indeed, tubule nano-crystals were visible *via* SEM after recrystallization on filter paper. The nano-roughness afforded by the tubules led to each of these waxes being able to achieve superhydrophobicity. On the natural leaf surfaces, ginkgo and katsura waxes have both exhibited near-superhydrophobicity.<sup>27,32</sup>

With maple wax achieving one of the lowest contact angles in the study (Fig. 6), and cedar wax achieving one of the highest, a very general link can be drawn between the relative abundance of co-crystallizing compounds and the contact angle of the re-crystallized waxes. However, this is not the only contributing factor, as smoketree wax has a slightly higher contact angle than cedar wax but a much lower relative abundance of co-crystallizing compounds.

SEM images revealed a difference in surface morphology, specifically nano-roughness, as a potential explanation for the difference in hydrophobicity between plant waxes (Fig. 6a–n). Carnauba, maple, and horsetail coated samples appeared smooth. However, ginkgo, katsura, cedar, and smoketree plant waxes recrystallized into tubules upon air drying and without heat treating (Fig. 6g–n), consistent with Jetter *et al.*<sup>33</sup>

In summary, the primary difference in hydrophobicity was that hydrophobic (90° < WCA < 150°) plant wax coatings were smooth and did not show nano-scale surface roughness, whereas superhydrophobic (WCA > 150°) samples contained wax tubules. Due to their high WCAs, we chose to focus further experiments on water-repellent coatings of waxes forming nanotubules based on nonacosan-10-ol. In this context, it was important to develop a scalable wax extraction process, so instead of using freshly picking leaves/needles off of trees, we used leaf litter from deciduous plant sources.

Among plant sources, we chose to focus on ginkgo because of its hydrophobicity, both observed on the leaf (Fig. 2) and filter paper samples (Fig. 6), and dense coverage of tubular microcrystalline wax aggregates (primarily made up of (*S*)-nonacosan-10-ol [(+)-ginnol]<sup>34–36</sup>) on both abaxial and adaxial surfaces.<sup>26</sup> The dense wax coverage was also observed in our results (Fig. 3). While cedar needles had greater hydrophobicity



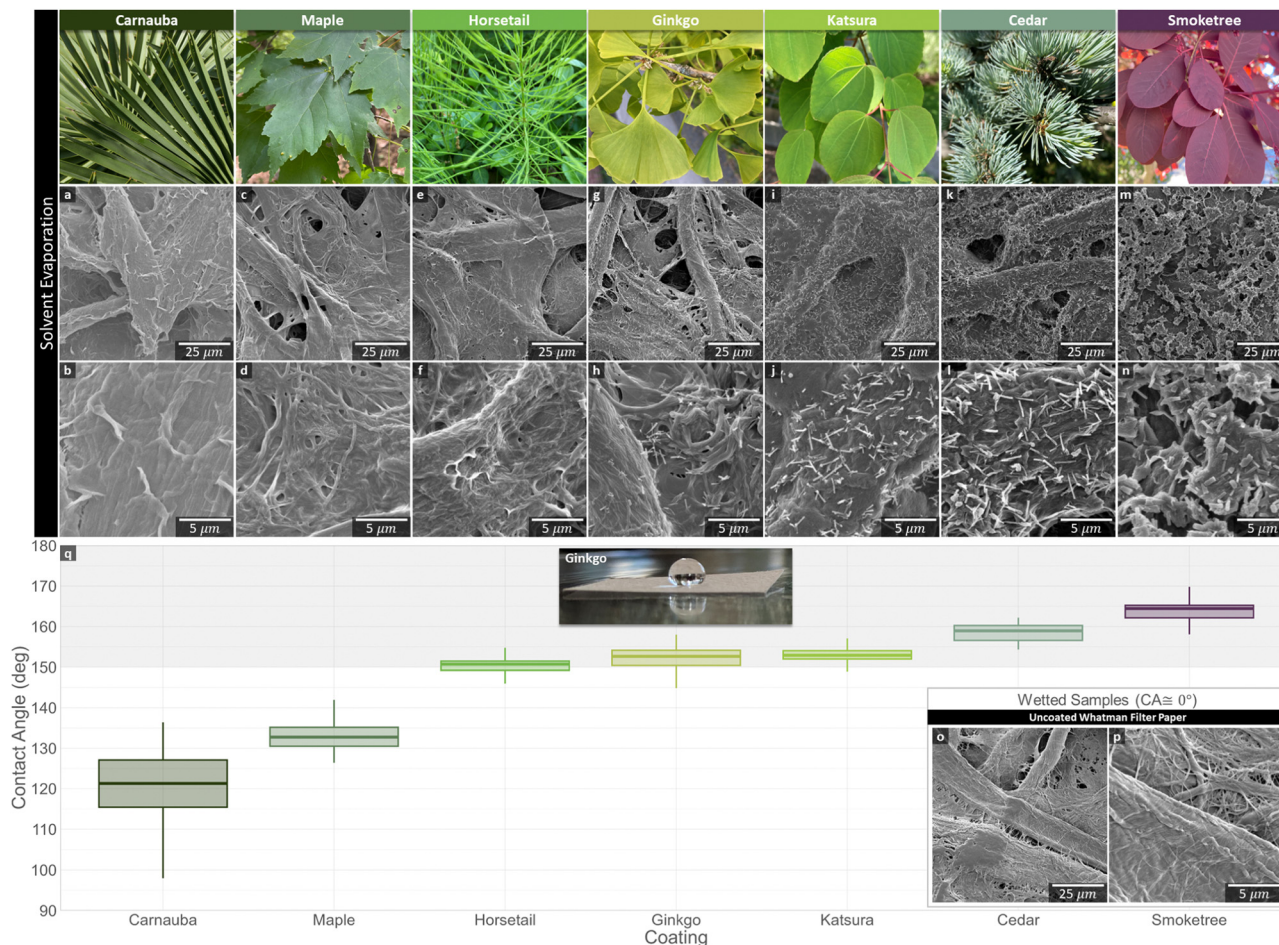


**Fig. 6** Plant wax survey of isolated wax recrystallized onto cotton-based filter paper and characterized using scanning electron microscopy (SEM) and water contact angle (WCA) measurements. (a)–(n) SEM images of filter paper with wax coatings by submerging the filter paper in a wax-solvent solution and air-drying, and (o) and (p) uncoated filter paper. (q) Tensiometer measurements showed all plant wax coated filter paper to be hydrophobic or superhydrophobic, while filter paper with no coating wetted immediately. All superhydrophobic samples contained a tubular wax morphology (g)–(n), while the remainder were more homogenous in appearance (a)–(f). Plant species: carnauba (*Copernicia prunifera*), maple (*Acer rubrum*), horsetail (*Equisetum arvense*, sterile shoots), ginkgo (*Ginkgo biloba*), katsura (*Cercidiphyllum japonicum*), cedar (*Cedrus atlantica*), and smoketree (*Cotinus coggygria*).

and wax coverage than ginkgo leaves, cedars are evergreens and therefore do not naturally lose their needles each year, in comparison to ginkgo leaves. Additionally, ginkgo leaves are already harvested for other commercial applications, specifically ginkgo is one of the most sold medicinal plants with a production of 8000 tons per year of dried leaves.<sup>37</sup> Therefore, we chose ginkgo wax for scale-up experiments testing water-repellent spray applications, in comparison with carnauba wax and commercial hydrophobic sprays.

### 3.3 Water-repellent spray: dispersion stability over time

In the following experiments, plant wax suspensions were compared against commercial coatings, prepared as instructed on their labels. The aqueous plant wax particle suspensions, containing either carnauba or ginkgo wax, were prepared with no additional emulsifiers and stabilizers. Bottles of commercial samples were shaken, as instructed. To maintain consistency, plant wax suspensions were also shaken, despite there being

visually very little sedimentation over the course of three months. After shaking, no sedimentation was visible with all samples looking similar (Fig. 11).

DLS was used to measure the stability of these suspensions with respect to surface charge. Within a day of preparation,  $\zeta$ -potentials were  $-57.0 \pm 1.5$  mV for carnauba and  $-52.3 \pm 0.5$  mV for ginkgo at a concentration of  $0.01 \text{ g mL}^{-1}$  (Table 1). Due to this net negative surface charge of wax particles, electrostatic double-layer repulsion was present and able to provide a high degree of stability for the suspension with no tendency to coagulate or flocculate.<sup>38</sup> Similar electrostatic charges were described by Lozhechnikova *et al.* as being caused by the amphiphilic nature of wax,<sup>6</sup> consisting of a hydrophobic tail attached to hydrophilic functional groups at the head (*e.g.*  $-\text{OH}$ ,  $-\text{COOH}$ ,  $-\text{CHO}$ ).<sup>39</sup> Upon melting and emulsifying in water, these amphiphilic molecules rearrange into micelles, resulting in a hydrophobic core and a hydrophilic particle surface interacting with the polar water phase.



**Table 1** Average (3 runs each) polydispersity index and zeta-potential of plant wax suspensions and commercial products. In all cases the PDI was less than 0.7 and therefore had a narrow enough size distribution for DLS. The zeta-potential of both Carnauba and ginkgo are close to  $-50$  and are therefore considered to have good stability

Material	Z-avg (nm)	PDI	$\zeta$ -potential (mV)	Time	Wax concentration ( $\text{g mL}^{-1}$ )
Coating 4	$169 \pm 3$	$0.082 \pm 0.019$	$57.3 \pm 0.4$	—	—
Carnauba	$168 \pm 1$	$0.103 \pm 0.018$	$-57.0 \pm 1.5$	1 day	0.01
Carnauba	$180 \pm 1$	$0.129 \pm 0.012$	$-65.0 \pm 1.6$	1 month	0.01
Carnauba	$201 \pm 1$	$0.173 \pm 0.017$	$-68.7 \pm 1.1$	1 day	0.015
Ginkgo	$184 \pm 0$	$0.134 \pm 0.016$	$-52.3 \pm 0.5$	1 day	0.01
Ginkgo	$188 \pm 1$	$0.119 \pm 0.007$	$-57.2 \pm 1.2$	1 month	0.01
Ginkgo	$264 \pm 1$	$0.283 \pm 0.011$	$-57.0 \pm 1.4$	1 day	0.015
Coating 1	$214 \pm 1$	$0.266 \pm 0.014$	$-52.0 \pm 1.9$	—	—
Coating 2	$184 \pm 2$	$0.214 \pm 0.014$	$61.6 \pm 1.0$	—	—
Coating 3	$666 \pm 10$	$0.352 \pm 0.035$	$66.9 \pm 0.8$	—	—

Time: time after suspension preparation, PDI: polydispersity index

The stability of the plant wax suspensions (ginkgo and carnauba) over storage time was also verified using DLS (Table 1). Although a slight increase in particle size was observed, all suspensions had good or excellent stability and showed reasonable particle size homogeneity with polydispersity indexes (PDI) close to 0.1. After a month, the Z-average increased from  $168.3 \pm 1.4$  nm (PDI = 0.103) to  $180.0 \pm 0.7$  nm (PDI = 0.129) for carnauba wax, and from  $184.3 \pm 0.2$  nm (PDI = 0.134) to  $188.4 \pm 0.5$  nm (PDI = 0.119) for ginkgo wax. Within this time, the intensity distributions decreased and broadened slightly, and the ginkgo and carnauba distributions became indistinguishable from one another, suggesting a stable state. Thus, the present work concludes that plant wax suspensions without emulsifiers can be stable, contrasting the findings of prior literature.<sup>7,40</sup>

Also observed was that particle size can be controlled by wax concentration (Table 1). With an increase in concentration from 0.10 to 0.15  $\text{g mL}^{-1}$ , the average particle size increased by 32.7 nm for carnauba wax and 79.4 nm for ginkgo wax. A similar finding was reported by Lozhechnikova *et al.*<sup>6</sup>

DLS measurements were also performed on commercial samples to compare against with plant wax suspensions (Fig. 7 and Table 1). All commercial products had a similar particle size to the plant wax suspensions except Coating 3, which had a bimodal distribution with particle size peaks at approximately 150 nm and 920 nm. As the Z-average increased, so did the PDI. All commercial products had a positive charge, except Coating 1, and a  $\zeta$ -potential with either good or excellent stability. Overall, all plant wax suspensions and commercial coatings, except Coating 3, were relatively similar and showed good or excellent stability with time.

### 3.4 The effect of thermal treatment on textile hydrophobicity

The effect of thermal treatment on coated fiber surface morphology and wettability was tested using SEM and WCA measurements. Because users would be heat treating their clothing in a home drying machine, our DSC data had to be compared with typical settings on these machines. The outlet thermostat set point on low heat is  $51.7$  °C (125 F) and on both medium and high heat is  $57.2$  °C (135 F). Additionally, the drum itself will reach a temperature of approximately  $62.8$  °C (145 F)

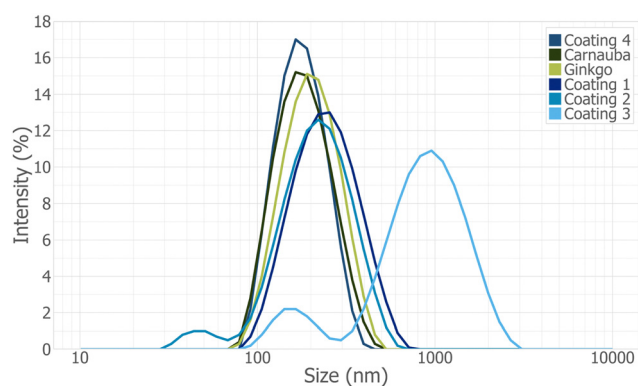


**Fig. 7** Dynamic light scattering (DLS) of  $0.01 \text{ g mL}^{-1}$  plant wax suspensions (carnauba and ginkgo) and commercial products (Coating 1–4), ordered from highest to lowest peak intensity. Plant wax suspensions were filtered beforehand using a  $0.45 \mu\text{m}$  diameter filter. Particle size using DLS, similar to.<sup>6</sup>

during operation.<sup>41</sup> This was in line with the temperature of textiles measured inside the drum with an IR gun (Milwaukee 10:1 Infrared Temp-Gun™) after running the GE dryer on medium heat in 5 min intervals for 30 min. Overall, the dryer set to medium heat thus reached temperatures near the ideal temperature of annealing wax coatings determined by DSC (see above), and in-line with Forsman *et al.* using a temperature of  $70$  °C.<sup>42</sup> Accordingly, our dryer was used at medium heat to prepare coatings for testing their performance on fabrics.

To monitor morphological changes of wax coatings during heat treatment, they were investigated using SEM (Fig. 8a–p, Table 2, and Fig. S7, ESI†). Ginkgo wax coatings appeared as small spheres (diameter  $852 \pm 0.402$  nm) when air dried, began to change morphology in the Tenney, and changed to tubules upon heating in the GE dryer. Coatings of carnauba wax remained as small spheres (diameter  $820 \pm 0.291$  nm) in all cases, but the number of spheres appeared to decrease and their diameter slightly increased when heated with the GE dryer. Therefore, some wax may have been partially melting and spreading on the surface, improving coverage and allowing molecular mobility. Both plant wax coatings appeared relatively rough in comparison to commercial coatings.



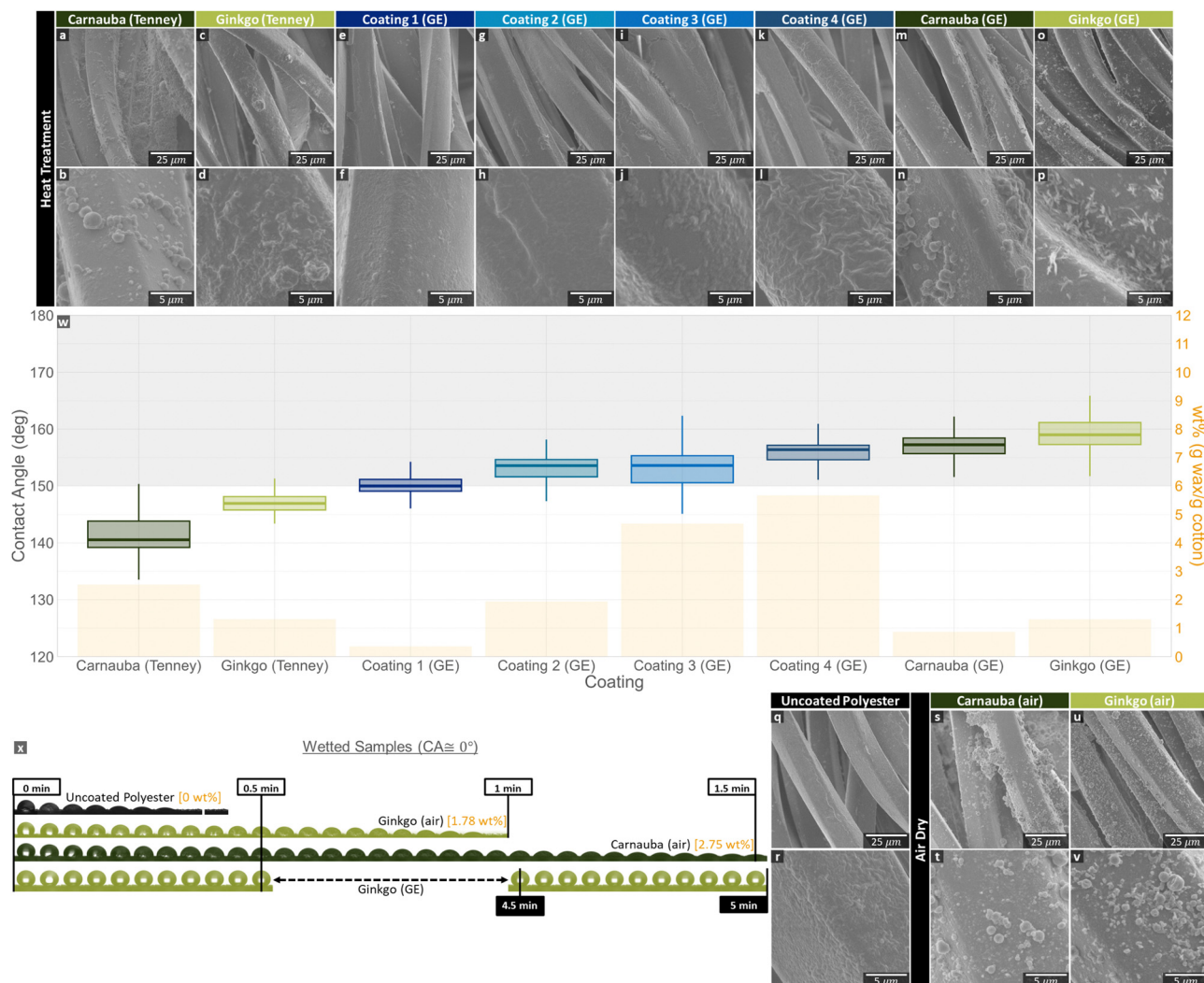


Fig. 8 Comparison of the morphology and hydrophobicity of plant wax suspensions (green) and commercial water repellent coatings (blue) sprayed onto polyester fabric and dried using various heat treatment methods or air. SEM images show the surface morphology of the polyester fabric uncoated (q) and (r) or coated and dried either with a Tenney: temperature humidity chamber (a)–(d), GE: home drying machine (e)–(p), or air dried (s)–(v). Static contact angle measurements (w) are shown as box plots and weight percent of coatings as orange bars, with still images from videos of wetted samples below (x).

Table 2 Particle sizes of coatings generated by different drying methods on polyester substrate

Wax source	Drying method	Diameter/length ( $\mu\text{m}$ )
Ginkgo	Air dry	$0.852 \pm 0.402$
Ginkgo	Tenney	Unmeasurable
Ginkgo	GE	$1.283 \pm 0.336$ by $0.157 \pm 0.042$
Carnauba	Air dry	$0.820 \pm 0.291$
Carnauba	Tenney	$0.924 \pm 0.451$
Carnauba	GE	$1.019 \pm 0.301$

The performance of hydrophobic coatings from commercial and plant wax sources on textiles was assessed using WCA measurements, with coatings, substrates, and drying methods compared. On the polyester substrate, ginkgo and carnauba samples heat-treated using the GE dryer had the highest WCAs and were superhydrophobic (Fig. 8). Additionally, three of the four commercial coatings were superhydrophobic. The fourth

commercial coating fell between hydrophobic and superhydrophobic. Carnauba and ginkgo samples heat-treated using the Tenney had hydrophobic WCAs. Samples that wetted within 5 min included polyester substrates that were either uncoated or coated with (air-dried) ginkgo or carnauba waxes. These samples are not shown on the WCA graph and are instead shown as a series of video frames to illustrate the behavior of droplets over time (Fig. 8x). For comparison, ginkgo heat-treated with a GE dryer is also shown in the video frames, which remained superhydrophobic for the full 5 min.

On the cotton substrate, ginkgo wax coatings heat-treated both using the Tenney and GE dryer had the highest WCA and were superhydrophobic (Fig. 9). For the commercial coatings applied to cotton, the order of hydrophobicity was the reverse of that on the polyester substrate. Coatings 1–3 were superhydrophobic, with Coating 1 (GE) having the highest WCA and Coating 3 the lowest. Coating 4 wetted within the 5 min,



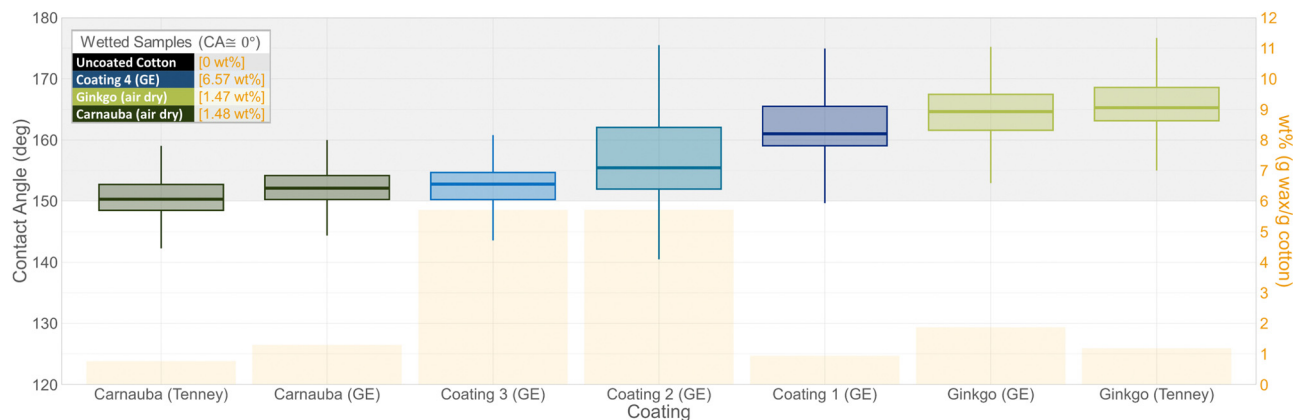


Fig. 9 Comparison of the hydrophobicity of plant wax suspensions (green) and commercial water repellent coatings (blue) sprayed onto cotton fabric and dried either with a Tenney: temperature humidity chamber, GE: home drying machine, or air dried. Wetted samples are shown in the inset box.

along with uncoated cotton, ginkgo wax (air dried), and carnauba wax (air dried). Both carnauba wax samples fell between hydrophobic and superhydrophobic.

WCAs can be further explained by local surface polarities as well as micro-reliefs. In making the dispersions, waxes become mobilized by heat and maximize their surface polarities upon cooling in the aqueous environment. It is therefore surmised that, upon melting of the wax, polar OH-groups become exposed as the tubules lose their structure, resulting in decreased hydrophobicity. The new structures are likely meta-stable at room temperature also after spraying/drying, and therefore may persist in “air-dried” controls. Finally, annealing again mobilizes the waxes, but this time they are exposed to air instead of water, leading to different structures now burying polar OH-groups and exposing non-polar hydrocarbons.<sup>6,43</sup> A similar, but chemically different, explanation has been given for carnauba wax by Lozhechnikova *et al.* and Forsman *et al.*<sup>6,42</sup>

In terms of micro-relief, various treatments, such as recrystallization from the melt or solution, tend to yield more or less smooth surfaces, due to their lower surface-to-volume ratios and, therefore, lower surface energies. Cheng *et al.*,<sup>44</sup> showed that melting of tubules does not affect the chemical composition or quantity of wax, suggesting that our wax treatments before annealing only resulted in loss of the nano-scale structure, formation of a smooth surface, and decrease in contact angle. After annealing, nonacosan-10-ol and nonacosanediols are thought to co-crystallize in tubular form.<sup>43</sup>

### 3.5 The effect of surface roughness on hydrophobicity of coated samples

In order for a surface to be superhydrophobic, low surface energy and high surface roughness must be present.<sup>45</sup> This allows for water to be suspended on both the substrate and pockets of air, reducing contact at the solid-liquid interface, and is referred to as the Cassie-Baxter state.<sup>10</sup> Among the substrates used here, surface roughness qualitatively increased from filter paper over polyester to cotton (Fig. 10). Ginkgo wax coatings, either recrystallized through solvent evaporation or annealing using the GE dryer, had WCAs increasing with substrate surface roughness (Fig. 6, 8, and 9).

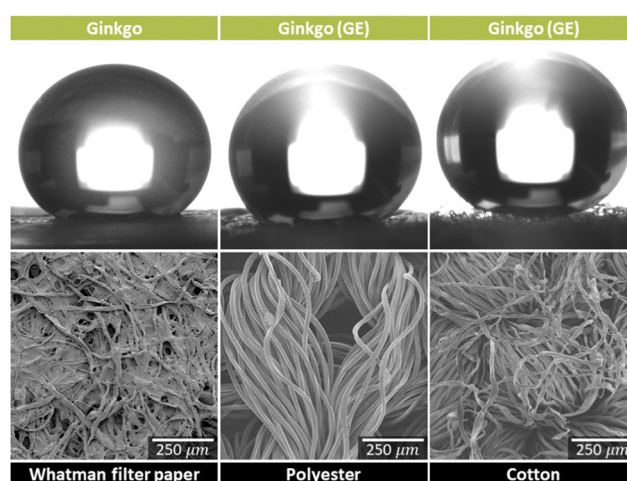
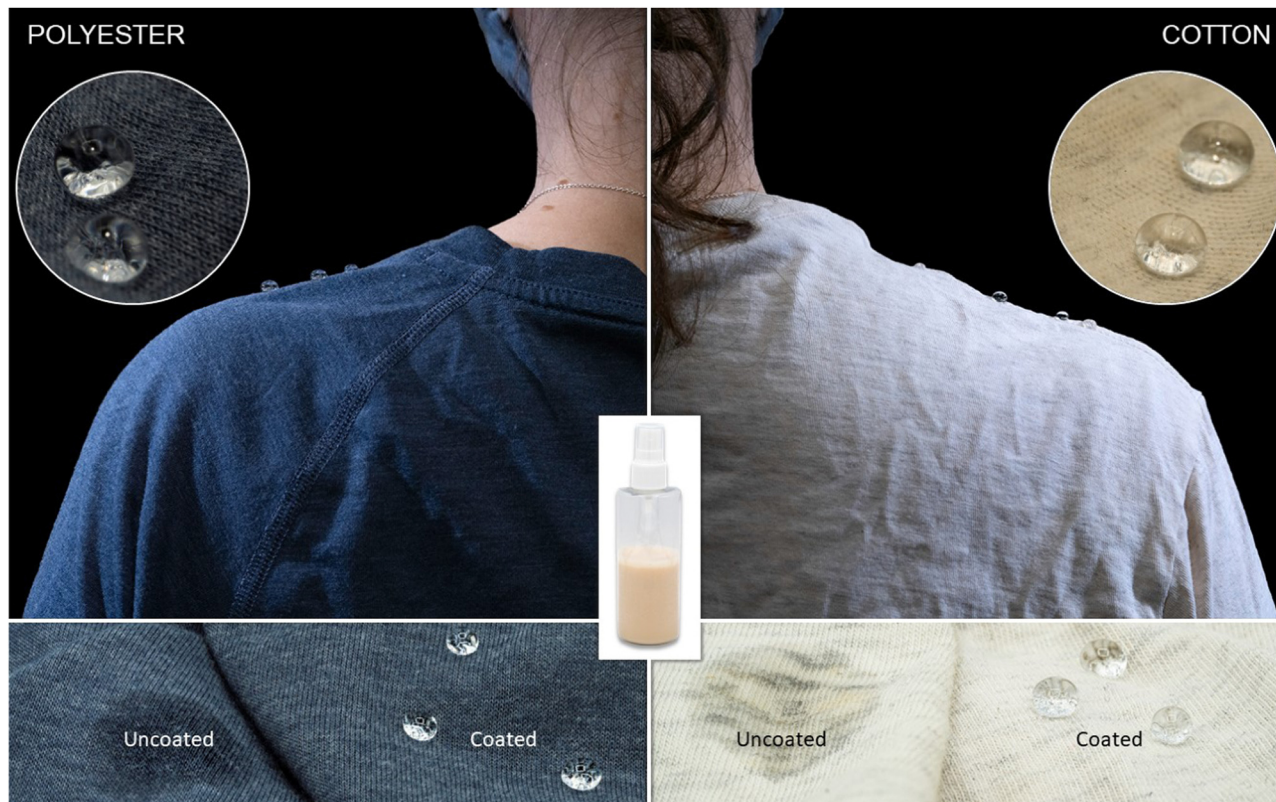


Fig. 10 The effect of substrate surface roughness on hydrophobicity. Surface roughness is shown with water contact angle (WCA) measurement images (coated with ginkgo wax) and scanning electron microscopy (SEM) images (uncoated) of Whatman filter paper, polyester, and cotton.

### 3.6 Scaling to t-shirt application

After confirming the ginkgo spray performed well compared to commercial coatings on small-scale fabric samples, we wanted to apply it to real-life applications by testing it on t-shirts. Polyester and cotton outdoor shirts were coated using the ginkgo wax spray, and water was applied to the surface to test the hydrophobicity (Fig. 11). Initially, the shirts were dried on medium heat for 30 min in a GE dryer, as had previously been done with fabric squares. However, shirts were not as hydrophobic as the textile samples discussed in Section 3.4. This was evident even before water fully absorbed into the textile because, as water drops began being absorbed by the textile, the base where the water drop made contact with the textile reflected the textile color, rather than appearing white (similar to the metallic appearance in Fig. 2). This change in color occurs when the air layer between the wax and water is no longer present. This appeared to be related to the increase in water content of the shirt vs. textile samples,





**Fig. 11** Polyester (left) and cotton (right) T-shirts sprayed with the water-repellent ginkgo wax spray and dried in the drying machine on medium heat for 60 min. The bottle in the center is the aqueous ginkgo wax suspension three weeks after being prepared. The bottom images are uncoated and coated sections of the T-shirts, demonstrating the hydrophobicity of the shirts after being coated.

resulting in a slower drying time. To test this, we dried the shirts for an additional 30 min (increasing the overall dry time to 60 min), which increased their hydrophobicity to the point that it was difficult to get photos of the water beaded on the person's shoulder rather than have it roll off. Thus, the Lotus effect was exhibited, rather than the Petal effect.

Qualitatively, the tactile feel and drape of the shirts were not affected by the water-repellent plant-based sprays. However, it was noticed that, if too much spray was added to a small section of the shirt, slight discoloration to a yellowish tint was present on the white shirt. Discoloration was not noticeable on the blue shirt. This was not a surprise given that the wax suspension had a yellowish tint. In future experiments we will investigate bleaching techniques and determine the optimal number of sprays to balance hydrophobicity and reduce discoloration.

The impact of wash-cycles on coating durability was not tested. However, this was investigated in previous work by Forsman *et al.*, in which their layer-by-layer carnauba wax coated textiles did not hold up to standard washing with detergents.<sup>42</sup> Instead, the coating would have to be reapplied after washing or used on clothing that is less frequently washed, such as outdoor clothing.<sup>42</sup> Therefore, it would be of interest to test the wash cycle durability of the ginkgo wax coated textiles in future work.

## 4 Conclusions

Aqueous plant wax suspensions were prepared by homogenization, without the addition of stabilizers or surfactants, to create PFC-free, petroleum-free hydrophobic coatings. This was achieved using wax from plant waste, with a focus on natural annual leaf-litter. These suspensions were then sprayed onto t-shirts and heat treated in home drying machines, using a similar procedure to that of commercial coatings that can be applied by the user at home. On both cotton and polyester textiles, the ginkgo wax produced a coating that was more hydrophobic than commercial products. In conclusion, a water-repellent spray was developed that could be applied by users at home, which was both more environmentally friendly than commercially available products and had greater water repellency.

## Author contributions

We strongly encourage authors to include author contributions and recommend using <https://casrai.org/credit/CRediT> for standardised contribution descriptions. Please refer to our general <https://www.rsc.org/journals-books-databases/journal-authors-reviewers/author-responsibilities/author-guidelines> for more information about authorship.



## Conflicts of interest

There are no conflicts to declare.

## Acknowledgements

The authors gratefully acknowledge the financial support provided by the NSERC Canfor Industrial Research Chair in Advanced Bioproducts, (#553449-19), NSERC Discovery Grant (RGPIN-2021-03172), the Canada Foundation for Innovation (Project number 022176), the Pacific Economic Development Canada (PacifiCan), and Natural Sciences and Engineering Research Council (Canada) Discovery Grants Program (grant #262461). The authors would also like to thank the UBC Bioimaging facility (RRID: SCR021304) for their technical assistance and use of their facilities.

## References

- 1 L. Ahrens, *J. Environ. Monit.*, 2011, **13**, 20–31.
- 2 M. P. Krafft and J. G. Riess, *Chemosphere*, 2015, **129**, 4–19.
- 3 P. J. Hill, M. Taylor, P. Goswami and R. S. Blackburn, *Chemosphere*, 2017, **181**, 500–507.
- 4 Arc'teryx, *ARC'TERYX AND PFCs*, <https://blog.arcteryx.com/arcteryx-and-pfc/>.
- 5 Patagonia, *Fluorinated DWR*, <https://www.patagonia.ca/our-footprint/dwr-durable-water-repellent.html>.
- 6 A. Lozhechnikova, H. Bellanger, B. Michen, I. Burgert and M. Österberg, *Appl. Surf. Sci.*, 2017, **396**, 1273–1281.
- 7 I. S. Bayer, D. Fragouli, P. J. Martorana, L. Martiradonna, R. Cingolani and A. Athanassiou, *Soft Matter*, 2011, **7**, 7939–7943.
- 8 Y. J. Liu, J. N. Shao and P. L. Liu, *IOP Conf. Ser.: Mater. Sci. Eng.*, 2018, **323**, 012013.
- 9 N. Forsman, A. Lozhechnikova, A. Khakalo, L.-S. Johansson, J. Vartiainen and M. Österberg, *Carbohydr. Polym.*, 2017, **173**, 392–402.
- 10 W. Wang, K. Lockwood, L. M. Boyd, M. D. Davidson, S. Movafaghi, H. Vahabi, S. R. Khetani and A. K. Kota, *ACS Appl. Mater. Interfaces*, 2016, **8**, 18664–18668.
- 11 P. Arlein, *Snow equipment wax formulation*, *U.S. Pat.*, 11059975B1, 2020, <https://patents.google.com/patent/US11059975B1/en?assignee=mountainflow>.
- 12 P. Arlein, *Snow equipment wax formulation*, *U.S. Pat.*, 11021633B1, 2020, <https://patents.google.com/patent/US11021633B1/en?assignee=mountainflow>.
- 13 E. Krendlinger, U. Wolfmeier, H. Schmidt, F.-L. Heinrichs, G. Michalczyk, W. Payer, W. Dietsche, K. Boehlke, G. Hohner and J. Wildgruber, *Waxes*, 2015, 1–63.
- 14 A. H. Warth, *The chemistry and technology of waxes*, 1947, <https://go.exlibris.link/jhNPM06k>.
- 15 R. Jetter, L. Kunst and A. L. Samuels, *Composition of Plant Cuticular Waxes*, Wiley Online Books, 2006, DOI: **10.1002/9780470988718.ch4**.
- 16 C. Neinhuis and W. Barthlott, *Ann. Bot.*, 1997, **79**, 667–677.
- 17 Y. Gaillard, A. Mija, A. Burr, E. Darque-Ceretti, E. Felder and N. Sbirrazzuoli, *Thermochim. Acta*, 2011, **521**, 90–97.
- 18 W. Zhang, P. Lu, L. Qian and H. Xiao, *Chem. Eng. J.*, 2014, **250**, 431–436.
- 19 M. Wen, C. Buschhaus and R. Jetter, *Phytochemistry*, 2006, **67**, 1808–1817.
- 20 M. Abramoff, P. Magalhães and S. J. Ram, *Biophotonics Int.*, 2003, **11**, 36–42.
- 21 C. Buschhaus and R. Jetter, *Plant Physiol.*, 2012, **160**, 1120–1129.
- 22 R. Jetter and M. Riederer, *Bot. Acta*, 1995, **108**, 111–120.
- 23 H. Wang, H. Shi, Y. Li, Y. Yu and J. Zhang, *Front. Environ. Sci. Eng.*, 2013, **7**, 579–588.
- 24 L. Schreiber and J. Schönherr, *Pestic. Sci.*, 1993, **38**, 353–361.
- 25 G. M. Hunt and E. A. Baker, *Chem. Phys. Lipids*, 1979, **23**, 213–221.
- 26 P.-G. Gülz, E. Müller, K. Schmitz, F.-J. Marner and S. Güth, *Z. Naturforsch., C: J. Biosci.*, 1992, **47**, 516–526.
- 27 H. Kang, P. M. Graybill, S. Fleetwood, J. B. Boreyko and S. Jung, *PLoS One*, 2018, **13**, e0202900–e0202900.
- 28 K. Koch and W. Barthlott, *Philos. Trans.: Math., Phys. Eng. Sci.*, 2009, **367**, 1487–1509.
- 29 T. W. Brakke, W. P. Wergin, E. F. Erbe and J. M. Harnden, *Remote Sens. Environ.*, 1993, **43**, 115–130.
- 30 P. J. Holloway, *J. Sci. Food Agric.*, 1969, **20**, 124–128.
- 31 E. Bormashenko, R. Pogreb, T. Stein, G. Whyman, M. Erlich, A. Musin, V. Machavariani and D. Aurbach, *Phys. Chem. Chem. Phys.*, 2008, **10**, 4056–4061.
- 32 C. Neinhuis and W. Barthlott, *New Phytol.*, 1998, **138**, 91–98.
- 33 R. Jetter and M. Riederer, *Planta*, 1994, **195**, 257–270.
- 34 A. Dommissé, J. Wirtz, K. Koch, W. Barthlott and T. Kolter, *Eur. J. Org. Chem.*, 2007, 3508–3511.
- 35 H. L. Casal and P. Moyna, *Phytochemistry*, 1979, **18**, 1738–1739.
- 36 P. J. Holloway, C. E. Jeffree and E. A. Baker, *Phytochemistry*, 1976, **15**, 1768–1770.
- 37 B. Singh, P. Kaur Gopichand, R. D. Singh and P. S. Ahuja, *Fitoterapia*, 2008, **79**, 401–418.
- 38 R. J. Hunter, *Zeta potential in colloid science: principles and applications*, 1981.
- 39 P. Wagner, R. Fürstner, W. Barthlott and C. Neinhuis, *J. Exp. Bot.*, 2003, **54**, 1295–1303.
- 40 Y. Wang, B. He and L. Zhao, *BioResources*, 2017, **12**, 7774–7783.
- 41 Haier, *Dryer - Explanation of Dryer Temperatures*, 2022, <https://products.geappliances.com/appliance/gea-support-search-content?contentId=20985>.
- 42 N. Forsman, L.-S. Johansson, H. Koivula, M. Tuure, P. Kääriäinen and M. Österberg, *Carbohydr. Polym.*, 2020, **227**, 115363.
- 43 H. J. Ensikat, P. Ditsche-Kuru, C. Neinhuis and W. Barthlott, *Beilstein J. Nanotechnol.*, 2011, **2**, 152–161.
- 44 Y. T. Cheng, D. E. Rodak, C. A. Wong and C. A. Hayden, *Nanotechnology*, 2006, **17**, 1359–1362.
- 45 S. Gorb, *Functional Surfaces in Biology: little structures with big Effects*, Springer, 2009, vol. 1.

